

RESEARCH

Open Access



# How successful is the CatBoost classifier in diagnosing different dental anomalies in patients via sella turcica and vertebral morphologic alteration?

Merve Gonca<sup>1\*</sup> , Busra Beser Gul<sup>1</sup>  and Mehmet Fatih Sert<sup>2</sup> 

## Abstract

**Background** To investigate how successfully the classification of patients with and without dental anomalies was achieved through four experiments involving different dental anomalies.

**Methods** Lateral cephalometric radiographs (LCRs) from 526 individuals aged between 14 and 22 years were included. Four experiments involving different dental anomalies were created. Experiment 1 included the total dental anomaly group and control group (CG). Experiment 2 only had dental agenesis and a CG. Experiment 3 consisted of only palatally impacted canines and the CG. Experiment 4 comprised patients with various dental defects (transposition, hypodontia, agenesis-palatally affected canine, peg-shaped laterally, hyperdontia) and the CG. Twelve sella measurements and assessments of the ponticulus posticus and posterior arch deficiency were given as input. The target was to distinguish between anomalies and controls. The CatBoost algorithm was applied to classify patients with and without dental anomalies.

**Results** In order from lowest to highest, the predictive accuracies of the experiments were as follows: experiment 4 < experiment 2 < experiment 3 < experiment 1. The sella area (SA) (mm<sup>2</sup>) was the most important variable in experiment 1. The most significant variable in prediction model of experiment 2 was sella height posterior (SHP) (mm). Sella area (SA) (mm<sup>2</sup>) was again the most relevant variable in experiment 3. The most important variable in experiment 4 was sella height median (SHM) (mm).

**Conclusions** Every prediction model from the four experiments prioritized different variables. These findings may suggest that related research should focus on specific traits from a diagnostic perspective.

**Keywords** Tooth abnormalities, Tooth, impacted, Algorithms, Machine learning, Orthodontics

\*Correspondence:

Merve Gonca  
mervegonca@gmail.com

<sup>1</sup>Faculty of Dentistry, Department of Orthodontics, Recep Tayyip Erdoğan University, Rize, Turkey

<sup>2</sup>Department of Business Administration (Quantitative Methods), Gaziantep University, Gaziantep, Turkey



© The Author(s) 2024. **Open Access** This article is licensed under a Creative Commons Attribution-NonCommercial-NoDerivatives 4.0 International License, which permits any non-commercial use, sharing, distribution and reproduction in any medium or format, as long as you give appropriate credit to the original author(s) and the source, provide a link to the Creative Commons licence, and indicate if you modified the licensed material. You do not have permission under this licence to share adapted material derived from this article or parts of it. The images or other third party material in this article are included in the article's Creative Commons licence, unless indicated otherwise in a credit line to the material. If material is not included in the article's Creative Commons licence and your intended use is not permitted by statutory regulation or exceeds the permitted use, you will need to obtain permission directly from the copyright holder. To view a copy of this licence, visit <http://creativecommons.org/licenses/by-nc-nd/4.0/>.

## Background

Lateral cephalometric radiographs (LCRs) are commonly used in orthodontic practice to diagnose, plan treatment, and assess skeletal maturation. Additionally, these radiographs can yield other diagnostic information of the skull, face, and upper cervical spine [1–3]. Previous researchers have investigated variations in the dimension and morphology of the sella turcica, deficiencies in the posterior arch, and the association of the ponticulus posterior with different syndromes, disorders, skeletal structures, and dental anomalies using LCRs [3–7].

The sella turcica is a saddle-shaped bone structure on the intracranial surface of the sphenoid bone body. It comprises the anterior and posterior walls called the tuberculum sella and dorsum sellae. The pituitary gland resides within the sella turcica, surrounded by anterior and posterior clinoid processes. The walls have distinct embryologic origins, with the anterior tied to dental epithelial progenitor cells and the posterior developing like a vertebral body under the influence of the notochord [8, 9].

The sella turcica bridge (STB) is a common morphologic variation resulting from posterior and anterior interclinoid ligament calcification or an anomaly occurring during the embryologic development of the sphenoid bone [1, 9–11]. This calcification process occurring during the developmental stages of the sella turcica can impact the surrounding structures, including dental tissues, leading to dental anomalies such as hypodontia, tooth transpositions, and palatal canine impaction [12]. These anomalies or variations of the STB, which can be detected during a standard orthodontic radiography examination, have previously been demonstrated in dental malformations, transposition, and tooth agenesis. Because of this developmental relationship and the sella turcica's ready visibility on LCRs taken routinely in orthodontic practice, several studies have investigated the size and anatomical deviations in the sella turcica and their associations with dental anomalies [3, 7, 9, 13]. The analysis of sella turcica dimensions, such as length and height, has been crucial in identifying potential correlations between sella turcica anomalies and dental anomalies like tooth agenesis and palatally impacted canines [12]. Moreover, sella turcica bridging, a common anomaly associated with dental abnormalities, has been correlated with alterations in sella turcica dimensions and morphology [14].

LCRs can also show common non-anatomic differences and morphologic anomalies, such as spina bifida, odontoid deformities, elongated styloid processes, and 1st cervical vertebral (CV) malformations (especially ponticulus posticus and posterior arch deficiency) [15]. The ponticulus posticus is a malformed bone bridge extending from the posterior part of the superior articular process

of the atlas and the posterolateral part of the upper edge of the posterior arch of the atlas, through which the vertebral artery passes [13, 16, 17]. Posterior arch deficiency is attributed to defective or incomplete development of the cartilage preformation of the arch rather than an ossification disorder [18]. The relationship between dental anomalies and ponticulus posticus and posterior arch deficiency can be attributed to the involvement of neural crest cells during development. Neural crest cells play a crucial role in the formation of both the anterior wall of the sella turcica and dental progenitor cells, which give rise to the teeth. This shared embryological origin suggests a potential link between skeletal variations such as ponticulus posticus and posterior arch deficiency and dental anomalies [9].

Machine learning, a subset of artificial intelligence (AI), involves computer learning by making inferences from data using various mathematical and statistical methods. Machine learning enables computers to increase their capabilities and performance by training on data, reducing the need for reprogramming. Additionally, machines may automatically perform various activities or tests based on their algorithms. Due to technological advances, regression, classification, clustering, and dimensionality reduction have been successfully used in medicine for diagnosis, treatment, and prognosis [19].

CatBoost, a machine learning algorithm developed by Yandex, derives its name from combining “Category” and “Boosting”. This open-source algorithm was created as a viable alternative to XGBoost and LightGBM, with the specific aim of enhancing the performance of Gradient Boosting [20]. CatBoost needs minimal hyperparameter adjustment to allow model developers to concentrate on other tasks. CatBoost's automatic feature priority ranking allows for finding important variables without intervention [21].

To our knowledge, no computer-aided method has been developed to detect dental anomalies via sella turcica measurements, and ponticulus posticus, and posterior arch assessments obtained from LCRs. Four experiments were created: (1) total dental anomalies-control group (CG), (2) solely agenesis-CG, (3) only palatally impacted canines-CG, (4) other anomalies (transposition, hypodontia, numerous dental anomalies, peg-shaped teeth, and hyperdontia)-CG. This study compared the success rates in detecting dental anomalies using the CatBoost classifier in all experiments. The variables with the most significant level of importance in each experiment were determined.

## Methods

This retrospective study was conducted in accordance with the ethics defined in the Declaration of Helsinki, and approval was obtained from Recep Tayyip Erdogan

University, Faculty of Medicine, Research Ethics Committee (Registration number: 2022/36). The study sample was selected through retrospective screening of LCRs and Panoramic Radiographs (PRs) of patients referred for treatment in the Department of Orthodontics, Faculty of Dentistry, Recep Tayyip Erdogan University. Informed written consent was obtained for each patient routinely at the beginning of treatment, including consent to use patient records in scientific studies.

The selection criteria of the total dental anomaly group (TDAG) and CG were as follows: (1) Turkish ethnicity; (2) no previous orthodontic treatment or surgery, an age range of 14–22 years; (3) good quality of LCRs and PRs; (4) clear visualization of the sella turcica and ponticulus posticus; (5) no cleft lip or palate, craniofacial anomalies, syndromes, systemic disorders, and severe mandibular deviation and history of facial trauma, head and/or neck surgery, radiotherapy, and chemotherapy; (6) no metal or motion artifacts in the images.

LCRs were obtained using a Planmeca Promax 2D S2 imaging unit (Planmeca Oy; Helsinki, Finland) with the following parameters: 66 kVp, 10 mA, 10.5 s. The patients were oriented with the sagittal plane perpendicular to the ground and the left side of the head toward the image receptor for LCRs. The canthomeatal line was parallelly aligned. Every LCR image contained a 45-mm calibration rod.

### Study group

Dental anomalies were diagnosed using pretreatment panoramic and LCRs, intraoral images, and orthodontic

dental castings. Additional diagnostic records, such as cone-beam computed tomography recordings, were also employed in individuals with palatally impacted canines. Patients with dental agenesis had only premolar agenesis regardless of region or only upper lateral agenesis or oligodontia. Patients with various and multiple dental anomalies (transposition, hypodontia, agenesis-palatally impacted canine, peg-shaped laterally, and hyperdontia) were included in the study.

Pretreatment records of 263 subjects with dental anomalies were selected to create TDAG. The distribution of the type of dental anomalies and sex are shown in Table 1. A total of 263 patients, 102 males, and 161 females, with skeletal class I malocclusion ( $0^\circ \leq ANB \leq 4^\circ$ ) and no dental anomalies (no supernumerary, missing or impacted teeth etc. except third molars), were selected from digital archives and examined as the CG.

### Measurements of the sella turcica and determination of the ponticulus posticus and posterior arch deficiency

Length, perimeter, area, and ratio measurements were performed in the sella turcica. Length measurements were made by modifying the measurements in Elnour et al. [22] and Sato and Endo's study [7]. Perimeter and area measurements were made according to the definitions in the study of Sato and Endo [7].

Two different methods in the literature were modified to evaluate the sella turcica bridge. The two previous methods made evaluations based on ordinal scoring, but we used ratios. The first method to quantify the degree of sella turcica bridging developed by Leonardi et al. [1] was used. This score was calculated from the ratio of the sella length (STL) to the sella diameter (SD) and defined as the ratio of STL/SD. The second method used was from the study of Sundareswaran and Nipun. This score was calculated from the ratio of the inter-clinoid distance (ID) to the STL and defined as the ratio of ID/STL [23]. Tables 2 and 3 explain the points and sizes of the sella turcica, and Figs. 1 and 2 demonstrate its points and sizes.

The extent of ponticulus posticus calcification on the atlas was classified as no calcification (no bony emergence), incomplete calcification (partial bony emergence), or complete calcification (complete bone bridge) (Fig. 3) [3].

Completion of the posterior arch of the atlas was evaluated as present or absent (Fig. 4) [9].

All measurements were performed using a computer system including an Image J analysis software program (version 1.51, National Institutes of Health, Bethesda, Maryland, USA). One observer performed all the tracing and measurements with 6 years of orthodontic experience (\*\*\*)

**Table 1** Distribution of dental anomalies

Dental Anomalies	fe- male (n)	male (n)	total (n)
Only Palatally Impacted canines <sup>a</sup>	58	14	72
Palatally Impacted canine*agenesis <sup>c</sup>	7	4	11
Palatally Impacted canine*peg shaped laterally <sup>c</sup>	1	2	3
Palatally Impacted canine*agenesis*peg shaped laterally <sup>c</sup>	1	0	1
Palatally impacted canine*transposition (other side) <sup>c</sup>	2	0	2
Only Agenesis <sup>b</sup>	79	51	130
Agenesis*peg shaped laterally <sup>c</sup>	16	3	19
Agenesis*transposition <sup>c</sup>	2	0	2
Only peg shaped laterally <sup>c</sup>	2	1	3
Only transposition <sup>c</sup>	7	4	11
Transposition*peg shaped laterally <sup>c</sup>	4	0	4
Only hyperdontia <sup>c</sup>	1	4	5
<b>Total</b> <sup>d</sup>	180	83	263

a; data used for the creation of the impacted canine group

b; data used for the creation of the agenesis

c; data used for the creation of the other anomaly group

d; data used for the creation of the total dental anomaly group

**Table 2** Definitions of the sella turcica points and used planes

Tuberculum sellae (TS)	The tip of the tuberculum sellae
Dorsum sellae (DS)	The most superior tip of the dorsum sellae
Sella turcica floor (SF)	The deepest point on the floor of pituitary fossa
Posterior inner wall of the pituitary fossa (PPF)	The deepest point of the posterior inner wall of the sella turcica
Anterior clinoid process (ACP)	The most posterior point of anterior clinoid process
Posterior clinoid process (PCP)	The most anterior point of posterior clinoid process
Sella anterior (SA)	The most anterior point of the sella
Sella posterior (SP)	The most posterior point of the sella
FH plane	The plane passing through the inferior margin of the orbit and the upper margin of the external auditory meatus
FH' plane	The plane crossing the sella floor parallel to the FH plane

**Table 3** Definitions of the sella turcica measurements

Sella length (STL) (mm)	The distance from TS to DS
Sella height median (SHM) (mm)	The distance between the point where the perpendicular descending from the midpoint of the TS and DS distance to the FH' plane intersects at FH' and the midpoint of the TS-DS distance
Interclinoid distance (ID) (mm)	The distance from ACP to PCP
Sella diameter (SD) (mm)	The distance from TS to PPF
Sella area (SA) (mm <sup>2</sup> )	The area included by the outline of the sella and capped by a line joining DS to TS
Sella perimeter (STP) (mm)	The perimeter of the area included by the outline of the sella and capped by a line joining DS to TS
Sella width distance (SW) (mm)	The distance between the projection points on FH' of the perpendiculars descending from the points SA and SP to the plane FH'.
Sella height anterior (SHA) (mm)	The distance between the TS and the point where the perpendicular descending from the TS to the TS to the FH' plane crosses the FH' plane.
Sella height posterior (SHP) (mm)	The distance between the DS and the point where the perpendicular descending from the DS to the DS to the FH' plane crosses the FH' plane.
Sella turcica depth (STDe) (mm)	The distance between the SF and the point where the perpendicular descending from SF to the DS-TS line intersects the DS-TS line.
Ratio of ID/STL	The ratio of the interclinoid distance to sella length
Ratio of STL/SD	The ratio of the sella length to sella diameter

**Statistical analysis**

Experiment 1 comprised TDAG (male: 83; female: 180) /CG (male: 102; female: 161) from 526 patient records. Test statistics regarding age and sex were used to evaluate experiment 1 only. Data normality and homogeneity were assessed using the Kolmogorov-Smirnov test for chronologic age. The TDAG and CG were compared using the Mann-Whitney U test regarding age. The

distribution of TDAG and CG by sex was evaluated using the Chi-square test. P-values of <0.05 were accepted as statistically significant. Descriptive statistics for quantitative variables in the study are presented in Table 4 using the mean and standard deviation, and qualitative variables are presented in Table 5 using the number of individuals.

The selection of samples in experiments 2, 3, and 4 was carefully performed, matching the chronologic age and sex of the anomaly groups and CGs to eliminate the effect of these variables. An orthodontist who did not perform any measurements made these selections, further ensuring the non-biased study design.

Experiment 2 included only dental agenesis (DAG only) and controls from 260 patient records. Patients with only palatally impacted canine (PICG only) and controls comprised experiment 3 from 144 patient records. Some patients in the DAG group had many dental anomalies. Experiment 4 included patients with various and multiple dental anomalies (transposition, hypodontia, agenesis-palatally impacted canine, peg-shaped laterally, hyperdontia) (other DAG)/CG from 122 patient records.

Sella turcica measurements and assessments of the ponticulus posticus and posterior arch deficiencies were given as input, which returned the predicted groups (anomaly-CG) accordingly. There were 14 variables in each experiment.

The study was conducted using the “CatBoost” package in the open-source R environment. Four different experiments (data sets) were created. The control and anomaly groups had equal numbers of samples in each experiment.

The evaluation of the CatBoost algorithm was conducted separately in each experiment to assess its application. To use supervised learning methods, all data sets were divided into two distinct sets: a training set accounting for 70% of the data and a test set representing the remaining 30%. In this manner, the machine learning methods employed could be effectively employed. The training datasets were used for the purpose of learning, and the test data set was used to monitor the success of the established model. Throughout the study, the models that possessed the most optimal hyperparameters were used.

models that possessed the most optimal hyperparameters were used.

To ensure the robustness of the predictive models developed using the CatBoost algorithm, a comprehensive validation process was implemented. The steps are detailed as follows:

1. Data Splitting: The dataset was divided into training and test sets, with 70% of the data used for training the model and the remaining 30% used for testing.

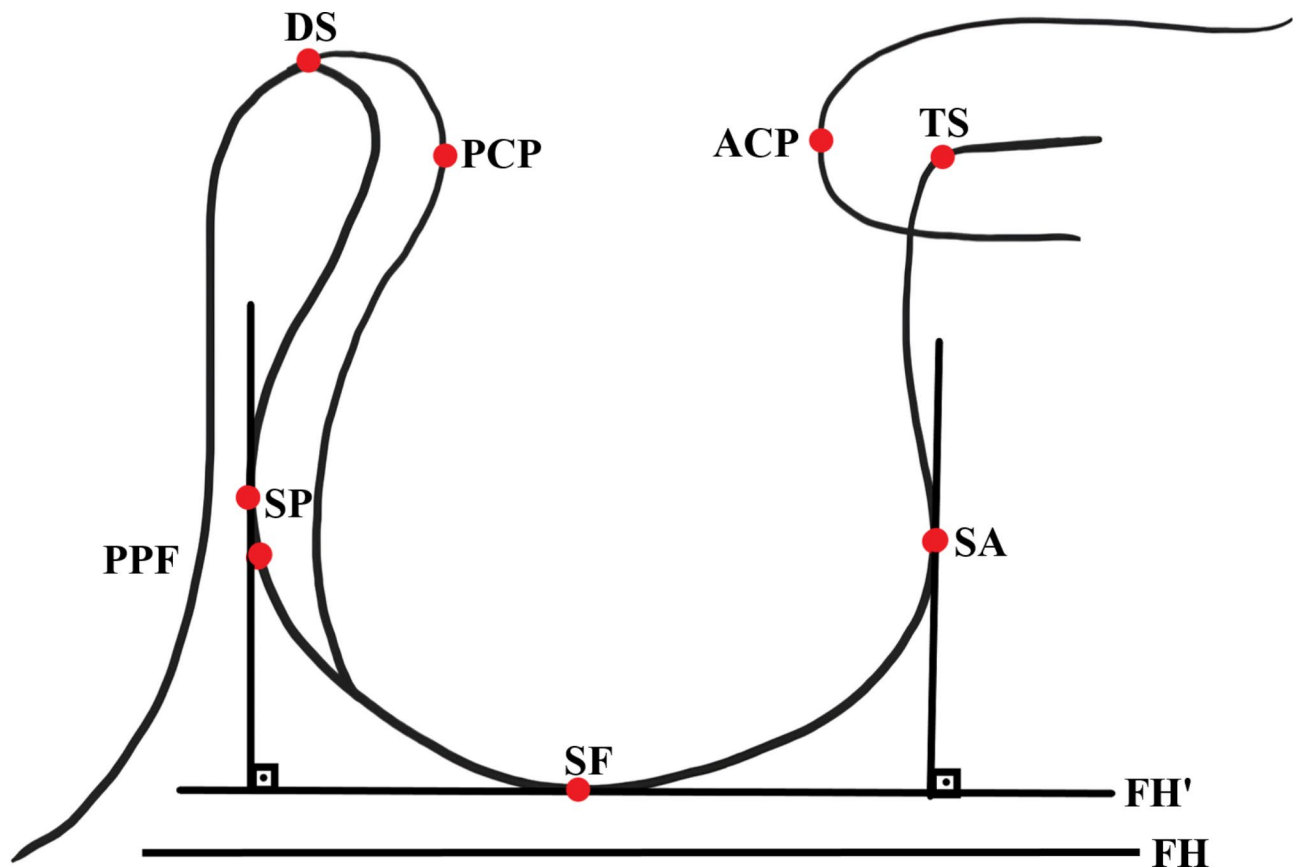


**Fig. 1** (TS) Tuberculum sellae, (DS) Dorsum sellae, (SF) Sella turcica floor, (PPF) Posterior inner wall of the pituitary fossa, (ACP) Anterior clinoid process, (PCP) Posterior clinoid process, (SA) Sella anterior, (SP) Sella posterior, (FH) Frankfurt horizontal plane, (FH') Frankfurt horizontal parallel plane

This split allows the model to learn from the training data and then be evaluated on unseen test data to assess its generalization performance.

2. **Cross-Validation:** A 5-fold cross-validation technique was employed to further validate the model's performance. In this approach, the training data was split into 5 subsets (folds). The model was trained on 4 folds and validated on the remaining fold. This process was repeated 5 times, with each fold being used as the validation set once. The results from the 5 folds were averaged to provide a more accurate measure of model performance.
3. **Performance Metrics:** Several performance metrics were calculated to evaluate the effectiveness of the CatBoost model. These performance criteria (Fig. 5):

**Precision:** The ratio of true positive predictions to the sum of true positive and false positive predictions.

**Recall:** The ratio of true positive predictions to the sum of true positive and false negative predictions.

**F1 Score:** The harmonic mean of precision and recall, providing a single metric that balances both.

These criteria were further elucidated through the use of the confusion matrix.

4. **Confusion Matrix:** The confusion matrix for each experiment was analyzed to understand the distribution of true positives, true negatives, false positives, and false negatives. This matrix helped in assessing the model's performance in distinguishing between different classes.
5. **Hyperparameter Tuning:** The CatBoost model was fine-tuned to identify the optimal set of hyperparameters that maximize its performance. This involved adjusting parameters such as learning rate, depth of trees, and number of iterations.

#### Measurement error

The measurements were performed on 144 randomly selected LCRs to assess the intra- and inter-rater reliability. The same operator with 6 years of orthodontic experience reassessed measurements 1 month after the first evaluation to test intra-rater repeatability. Another orthodontist with 10 years of orthodontic experience assessed randomly selected LCRs for inter-rater reliability.

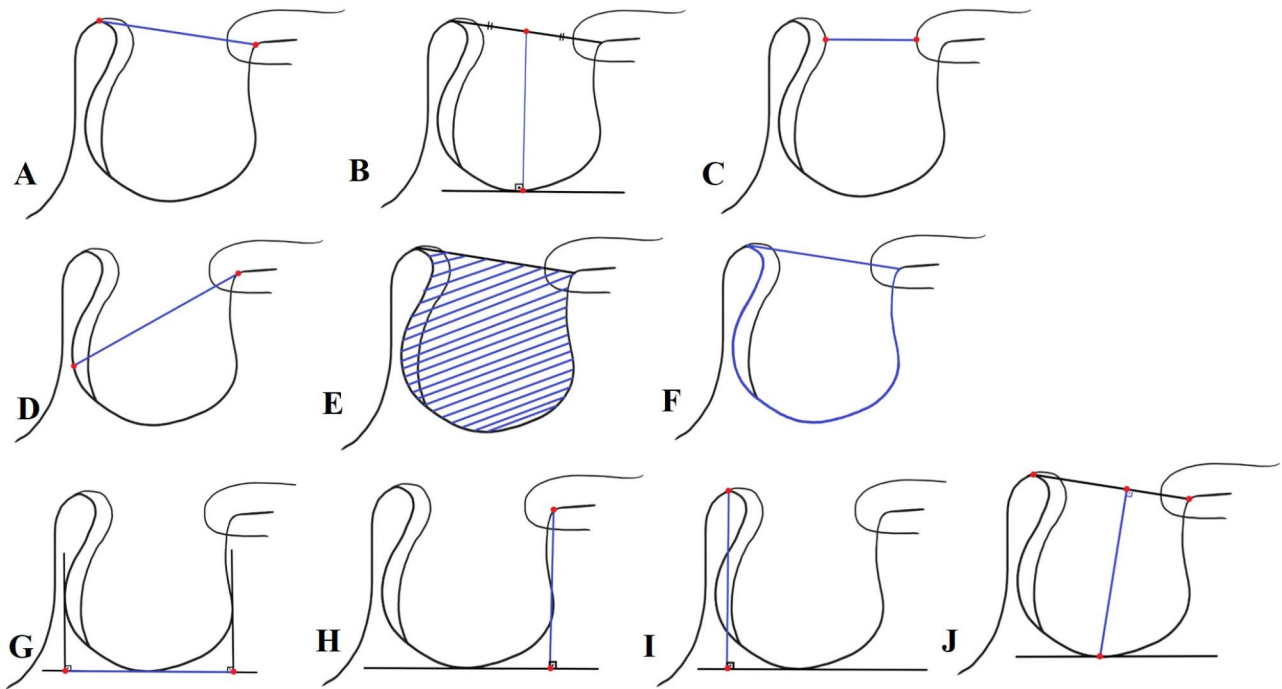


**Fig. 2** (A) Sella length (STL) (mm). (B) Sella height median (SHM) (mm). (C) Interclinoid distance (ID) (mm). (D) Sella diameter (SD) (mm). (E) Sella area (SA) (mm<sup>2</sup>). (F) Sella perimeter (STP) (mm). (G) Sella width distance (SW) (mm). (H) Sella height anterior (SHA) (mm). (I) Sella height posterior (SHP) (mm). (J) Sella turcica depth (STDe) (mm)

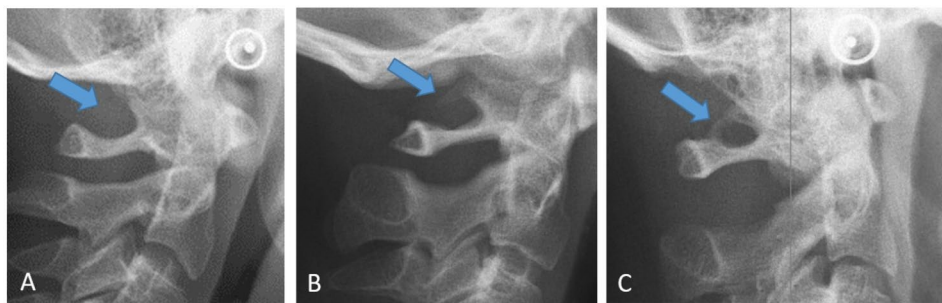


**Fig. 3** Demonstration of ponticulus posticus calcification on the atlas **A**: no calcification (no bony emergence), **B**: incomplete (partial bony emergence), **C**: complete (complete bone bridge)

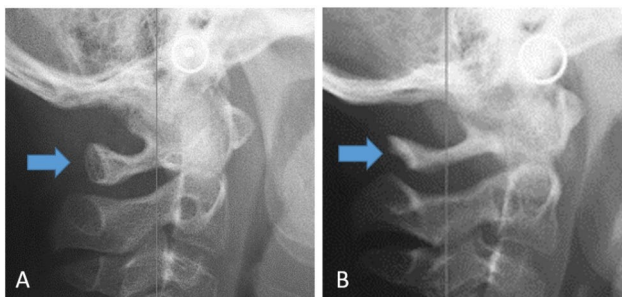


**Fig. 4** Completion of the posterior arch of the atlas (A) present, (B) absent

**Results**

In experiment 1, no statistically significant difference was found in the distribution of the anomaly and control groups according to sex ( $p=0.083$ ). There was

no statistically significant difference in age between the anomaly and control groups in both sexes (males;  $p=0.21$ ; females;  $p=0.58$ ).

Both intraobserver and interobserver reproducibility for posterior arch deficiency was 0.796 (95% CI: 0.633 to 0.960) indicating substantial reliability. The intraobserver and interobserver reproducibility for ponticulus posticus was 0.900 (95% CI: 0.835 to 0.965) and 0.834 (95% CI: 0.754 to 0.914), respectively, indicating excellent reliability [24]. The agreement between the first and second measurements in intra-observer reliability had excellent reliability for all sella measurements ( $ICC \geq 0.902$ ). The inter-observer reliability had excellent for all sella measurements except sella width distance ( $ICC \geq 0.896$ ) [25].

**Table 4** Descriptives in experiments

	Experiment 1		Experiment 2		Experiment 3		Experiment 4									
	TDAG (n = 263)		CG (n = 263)		Only DAGG (n = 130)		CG (n = 72)									
	Mean	SD	Mean	SD	Mean	SD	Mean	SD								
Age	16.3	1.49	16.24	1.48	16.33	1.57	16.31	1.47	16.3	1.48	15.99	1.07	16.25	1.36	17.37	1.91
Sella area (SA) (mm2)	67.38	15.82	66.79	16.49	65.65	16.62	65.77	15.21	72.6	14.94	68.59	18.55	64.89	13.77	66.77	19.76
Sella perimeter (STP) (mm)	32.39	3.69	32.12	3.81	31.85	3.86	31.93	3.65	33.81	3.27	32.37	4.05	31.85	3.38	32.25	4.4
Sella length (STL) (mm)	9.58	1.66	9.42	1.77	9.48	1.7	9.4	1.79	9.86	1.6	9.32	1.47	9.48	1.62	9.32	1.52
Sella height posterior (SHP) (mm)	8.54	1.4	8.18	1.46	8.52	1.52	8.1	1.4	8.69	1.45	8.19	1.45	8.38	1.04	8.12	1.56
Sella height anterior (SHA) (mm)	8.05	1.41	7.84	1.45	7.98	1.48	7.7	1.51	8.31	1.43	8.14	1.29	7.9	1.19	7.71	1.51
Sella height median (SHM) (mm)	8.29	1.17	8.01	1.22	8.25	1.28	7.9	1.22	8.5	1.15	8.17	1.15	8.14	0.87	7.92	1.29
Interclinoid distance (ID) (mm)	2.31	1.78	2.67	1.82	2	1.84	2.74	1.85	2.71	1.74	2.66	1.6	2.5	1.59	2.45	1.88
Sella diameter (SD) (mm)	11.67	1.5	11.56	1.63	11.66	1.67	11.64	1.72	11.91	1.3	11.64	1.31	11.39	1.3	11.37	1.5
Sella width distance (SW) (mm)	10.3	1.39	10.19	1.48	10.22	1.52	10.31	1.52	10.66	1.15	10.1	1.19	10.04	1.31	9.98	1.36
Sella turcica depth (STD <sub>e</sub> ) (mm)	8.2	1.16	7.94	1.24	8.17	1.31	7.86	1.2	8.35	1.12	8.07	1.21	8.1	0.82	7.88	1.31
ratio of ID/STL	0.24	0.18	0.28	0.18	0.21	0.19	0.29	0.18	0.28	0.18	0.28	0.16	0.26	0.15	0.27	0.19
Ratio of STL/SD	0.82	0.12	0.82	0.13	0.82	0.12	0.81	0.13	0.83	0.12	0.8	0.12	0.83	0.12	0.82	0.11

Tables 6 and 7 show the CatBoost results. Table 6 shows confusion matrices of the algorithm's predictions from each experiment. Table 7 displays the performance criteria that pertain to the accuracy of the predictions, which were obtained in an all-encompassing manner for each distinct experiment set. All these outputs are examined together to understand the study's results.

Based on the confusion matrices in Table 6, the results of each experiment can be interpreted as follows: In experiment 1, for TDAG and CG classes, the correct prediction rate (true positive) for TDAG was 32, and the false positive rate was 22. For CG, the correct prediction (true negative) was 31, and the false-negative rate was 22. This finding shows that the model had a balanced performance in recognizing both classes. In experiment 2, only for DAGG and CG, the correct prediction rate of DAGG was 19, and the false-positive rate was 11; the correct prediction rate of CG was 15, and the false-negative rate was 7. In this experiment, the model performed better in recognizing the DAGG class. In experiment 3, only for PICG and CG, the correct prediction rate of PICG was 10, and the false-positive rate was 6; the correct prediction rate of CG was 9, and the false-negative rate was 6. This finding indicates that the model showed a balanced performance between classes, but the number of samples was low. Moreover, in experiment 4, for the other DAG group and CG, DAG had a correct prediction rate of 9 and a false-positive rate of 4; the CG had a correct prediction rate of 9 and a false-negative rate of 4. The model also showed a balanced performance in this experiment.

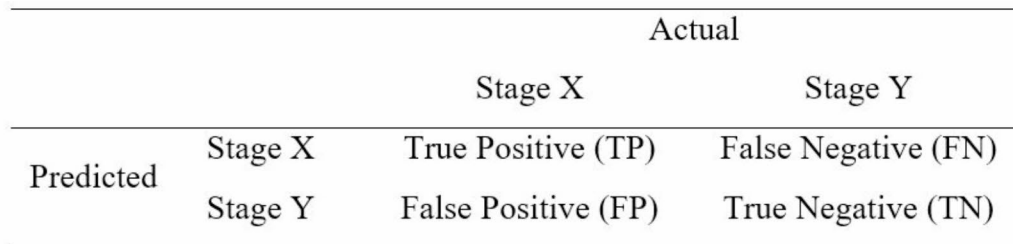
When the performance criteria (Table 7) are analyzed, it is seen that experiments 2 and 4 have the highest performance with 73% and 70.3% recall rate, respectively. This indicates that the model was more successful in recognizing true positives in these experiments. In terms of precision, experiment 4 had the highest value (74.1%), indicating that the model best discriminated false positives. The F1 score indicates the balance between precision and recall of the model. In this regard, experiment 4 (71.2%) and experiment 2 (68.6%) showed the best balanced performance.

The results obtained from the 5-fold cross-validation showed consistent performance across all folds, indicating the model's stability and reliability. The confusion matrices in Table 6 illustrate the distribution of predictions and actual values, providing insight into the model's ability to distinguish between anomaly and control groups. The performance metrics summarized in Table 7 further demonstrate the model's precision, recall, and F1 scores. These metrics confirm the robustness of the CatBoost classifier in predicting dental anomalies across different experiments.

In conclusion, these results show that the CatBoost model exhibits varying performances in different

**Table 5** Distribution of the vertebral assessments in all experiments

	Anomaly group					Control group				
	Ponticulus posticus			Deficient posterior atlas arches		Ponticulus posticus			Completion of the posterior arch	
	No	Incomplete	Complete	Complete	Deficient	No	Incomplete	Complete	Complete	Deficient
Experiment 1	127	91	45	246	17	113	112	38	240	23
Experiment 2	66	41	23	121	9	54	59	17	117	13
Experiment 3	28	30	14	69	3	39	20	13	68	4
Experiment 4	33	20	8	56	5	30	22	9	56	5



$$Precision = \frac{TP}{TP+FP} \quad Recall = \frac{TP}{TP+TN} \quad F1 \text{ score} = 2 * \frac{precision*recall}{precision+recall}$$

**Fig. 5** Performance metrics

**Table 6** Confusion matrices

Experiment 1	<b>TDAG</b>		<b>CG</b>
	Predicted		
TDAG	Actual	32	22
CG		22	31
Experiment 2	<b>Only DAGG</b>		<b>CG</b>
	Predicted		
Only DAGG	Actual	19	11
CG		7	15
Experiment 3	<b>Only PICG</b>		<b>CG</b>
	Predicted		
Only PICG	Actual	10	6
CG		6	9
Experiment 4	<b>Other DAG</b>		<b>CG</b>
	Predicted		
Other DAG	Actual	9	4
CG		4	9

**Table 7** Performance Criteria regarding the Accuracy of the prediction

	Precision	Recall	F1
Experiment 1	0.590	0.597	0.592
Experiment 2	0.648	0.730	0.686
Experiment 3	0.625	0.625	0.627
Experiment 4	0.741	0.703	0.712

experiments, but overall has a balanced performance and good accuracy. Experiment 4 stands out as the best performing experiment, especially in terms of accuracy and F1 score.

After applying the CatBoost algorithm in the study, the coefficients of each variable were obtained while reaching the highest prediction level. These variables show which of the independent variables are important in explaining the dependent variable for each experiment. The coefficients of the variables are presented in Fig. 6. The graph shows the name of each variable and the bars representing the degree of their contribution to the prediction model. The length of these bars indicates the importance of the variable in the model.

In experiment 1, the most important variable in the model was labelled “sella area (SA) (mm2)” and had the highest importance with a coefficient value close to 20, followed by “ratio of STL/SD” and “ratio of ID/STL”. The coefficients of these variables were around 17 and 12, respectively. The variables “sella height anterior (SHA) (mm)” and “interclinoid distance (ID) (mm)” also seemed to have significant contributions. On the other hand, the effect of variables such as “sella diameter (SD) (mm)” and “sella height posterior (SHP) (mm)” on the model could be considered relatively low or even insignificant with a coefficient value around 0.

In the prediction model developed for experiment 2, the most important variable was stated as “sella height posterior (SHP) (mm)”, followed by “interclinoid distance (ID) (mm)”. In this model, the effect of variables such as “sella diameter (SD) (mm)” and “sella turcica depth (STDe) (mm)” on the model was relatively low, but because their coefficients were not 0, they were not considered insignificant.



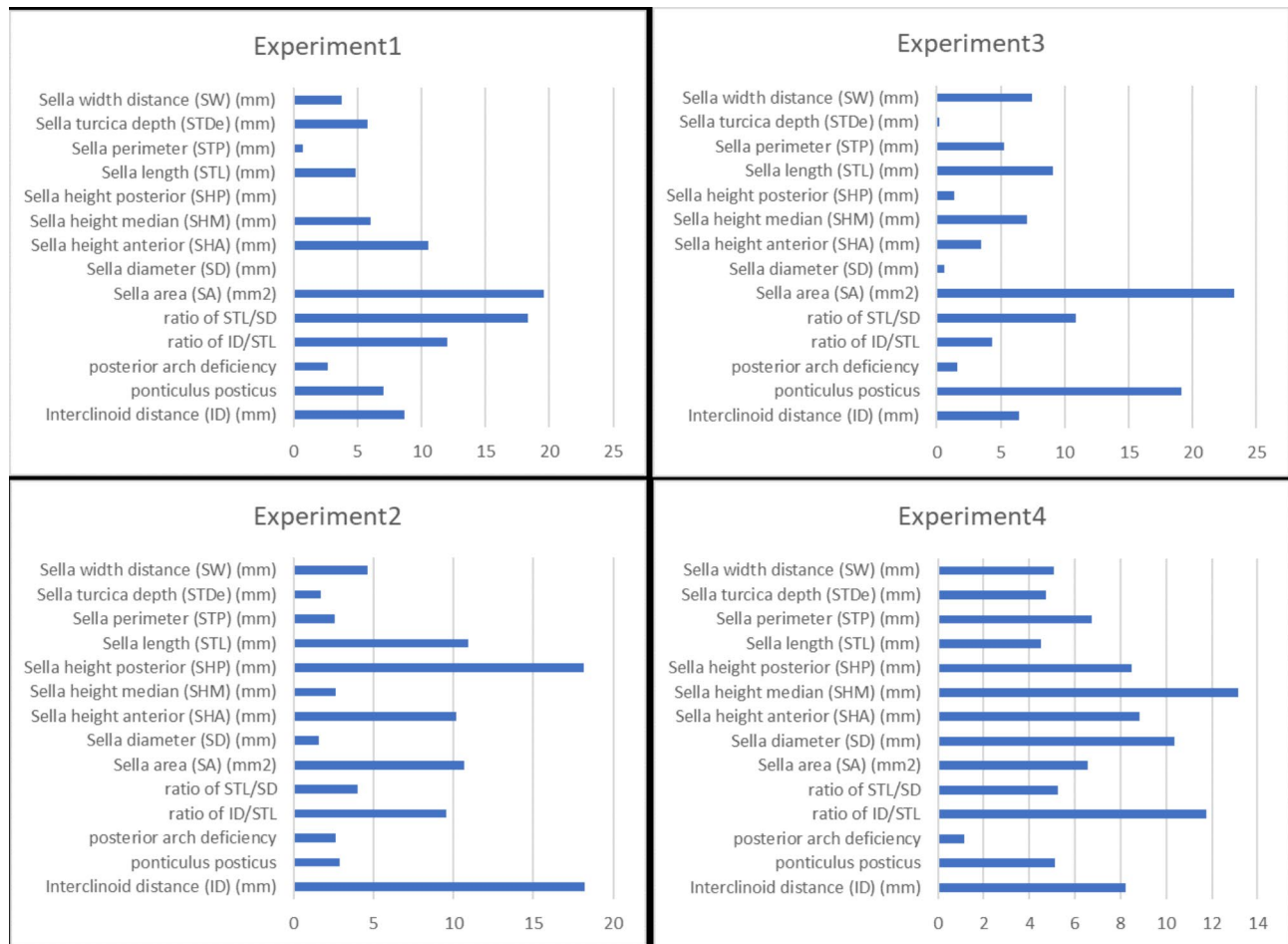


**Fig. 6** Representation of the importance level of variables for all experiments

In the model developed for experiment 3, “sella area (SA) (mm<sup>2</sup>)” was again the most important variable, followed by “ponticulus posticus” and “ratio of STL/SD”. In this model, similar to experiment 2, the effect of variables such as “sella diameter (SD) (mm)” and “sella turcica depth (STDe) (mm)” on the model could be considered relatively low or even insignificant with a coefficient value of 0.

The most important variable in the model developed for experiment 4 was “sella height median (SHM) (mm)”, followed by “ponticulus posticus” and “ratio of ID/STL”. In this model, unlike the others, almost all variables had a high coefficient, but the least contributing variable was “posterior arch deficiency”.

**Discussion**

The anterior wall of the sella turcica, dental epithelial progenitor cells, and the maxillary, palatal, and frontonasal developmental areas all originate from neural crest cells during embryonic development [9, 26, 27]. These structures also share common genes, such as the

homeobox (HOX) gene and the sonic hedgehog gene, which play a role in their development.

STB arises due to excessive ossification of the dura mater between the anterior and posterior clinoid processes [28]. This ossification process occurring during the developmental stages of the sella turcica can impact the surrounding structures, including dental tissues, leading to dental anomalies such as hypodontia, tooth transpositions, and palatal canine impaction [12]. Studies have investigated the predictive importance of sella turcica bridging and the measurements of length, height, circumference, and area of the sella turcica in identifying dental anomalies [28, 29].

The development of the neck and shoulder skeleton, including the ponticulus posticus and posterior atlas arches, is controlled by neural crest cells throughout fetal development [9]. Therefore, alterations throughout the developmental stage may cause the calcification of the sella turcica and ponticulus posticus and deficient posterior atlas arch, resulting in dental anomalies.

Different radiographic methods have been employed to study sella turcica dimensions and craniofacial

morphology. Some studies have examined the length, depth, and diameter of the sella turcica in patients with skeletal class 1, 2, and 3 malocclusions using LCRs. Based on these findings, only patients with skeletal class I malocclusion were selected as the CG for the present investigation because there may be differences in sella length, depth, diameter, and bridging in different skeletal classes [2, 30–33].

Research comparing the size of the sella turcica in relation to sex has shown contradictory findings. Many investigations found no significant differences between female and male individuals [2, 11, 34], but Magat et al. [31] reported a larger sella turcica width of the in women than in men. Conversely, Axelsson et al. [35]. found that men had longer sella turcicas than women. Longitudinal data on growth-related variations in sella turcica sizes indicate that the anterior wall remains stable, whereas the posterior wall exhibits resorptive alterations [36]. Based on the findings mentioned above in the literature, to eliminate age- and sex-related changes, we carefully matched the chronologic ages and sexes of the patients in the anomaly groups and CGs.

In the four experiments, the difference between the anomaly groups and CG was highlighted by the sella area, sella height median, posterior, ratio of STL/SD, and the ratio of ID/STL and ID. In comparing impacted canines and the CG (experiment 3), ponticulus posticus, which was low in importance in other groups, was the variable with a secondary level of importance. These findings show that different variables may be at the forefront of different dental anomalies. The size and diversity of data are of great importance for machine learning methods [37, 38]. In our study, the best accuracy values were obtained in experiments 4 and 2, respectively. Although experiment 4 had the fewest samples compared with other experiments, it obtained the best differential diagnosis.

The relationship between sella area measurement and dental anomalies has been discussed in a few studies in the literature [7, 39]. Studies comparing dental anomalies and CG were conducted by evaluating the sella turcica bridge rather than the sella area and height measurements [5]. Some studies reported that tooth agenesis, maxillary canine impaction, and tooth transposition had a common genetic origin and were associated with sella bridging [3, 7, 27, 40]. Assessment of the sella bridge is generally considered ordinal data, and researchers use different classification methods. Leonardi et al. [1]. divided the sella turcica bridge degrees into three groups. This score was calculated using the ratio of STL/SD. The definition of the “tip of the dorsum sellae,” which determines the length, differs among studies. Some studies, like ours, define the tip as the most superior tip of the dorsum sellae [23, 39]. However, others considered the

sella length the closest distance between the tuberculum and dorsum sellae [9, 27, 41]. Omastova et al. [39]. reported that using the closest distance between the tuberculum sella and dorsum sellae to evaluate calcification might underestimate length and overestimate partial bridging. For this reason, they evaluated the dorsum sellae point as the most superior tip of the dorsum sellae. In our study, dorsum sellae was based on the exact definition of Omastova et al. [39]. The distance from the dorsum sellae tip to the tuberculum sella does not always indicate the degree of calcification between the anterior and posterior clinoid processes. Hence, the present research also used Sundareswaran and Nipun’s method. In this method, the interclinoid distance indicates the different degrees of calcification of clinoid processes [23]. Our study evaluated the bridge of the sella turcica through these methods’ ratios, similar to the study of Omastova et al., to eliminate this confusion.

Experiment 1 evaluated the comparison of all dental anomaly samples with all controls. Although there was no statistically significant difference in the anomaly group and CG regarding age distribution and sex variables, sex distributions were heterogeneous compared with the other experiments. For this reason, lower accuracy values may have been obtained compared to other experiments. In experiment 1, the sella area, the ratio of STL/SD, and the ratio of ID/STL were the most important variables in distinguishing between total DAG and the CG, respectively.

Siddalingappa et al. [42]., in their study investigating the relationship between different dental anomalies and CG, stated a significant relationship between sella turcica bridging and dental anomalies. A small ratio of ID/STL meant that the amount of bridging was high. In our study, the ID/STL ratio, which had the second-highest significance level, showed increased bridging in the anomaly group.

Experiment 2 was designed to focus specifically on individuals with dental agenesis and controls. The abnormality group included individuals with either unilateral or bilateral lateral agenesis, one or more premolar agenesis regardless of location, or oligodontia with at least one missing lateral/premolar tooth. The results of experiment 2 demonstrated that the anomaly group was characterized by longer SHP and shorter ID compared with the CG.

Scribante et al. [41]. demonstrated that individuals with absent maxillary lateral incisors or mandibular second premolars showed no significant differences in the ID compared with the CG. Sato and Endo [7] stated that regardless of age, there was no significant difference in the ID or the prevalence of sella turcica bridging between patients with agenesis of the mandibular second premolar and those without tooth agenesis. However, patients

with severe tooth absences had one or two congenitally missing maxillary second premolars. They reported that agenesis of the upper second premolars and numerous missing teeth caused short ID. Although our findings contradicted Scribante et al., they were partially compatible with Sato and Endo. The main difference in our study was that our anomaly group consisted of a more heterogeneous sample, which made direct comparison difficult.

In experiment 3, the sella area, ponticulus posticus, and ratio of the STL/SD played the most significant roles in distinguishing between PICG only and the CG. A longer length in patients in PICG only compared with the CG in our study was inconsistent with previous investigations [27, 43]; however, our findings were partially in line with the study of Omastova et al. The sella area increased significantly in patients with only PICG, similar to the study of Omastova et al. [39]. Leonardi et al. and Ghadimi et al. [9, 26]. found that patients with palatally displaced canines had a higher occurrence of complete and incomplete ponticulus posticus than control subjects. In our investigation, the number of complete ponticulus posticus was almost the same between the anomaly and control groups. Nevertheless, our results regarding incomplete ponticulus posticus were similar to those of Leonardi et al. and Ghadimi et al. [9, 26]. Leonardi et al. [26]. found that subjects with palatally displaced canines had more deficient posterior arches than the controls. However, Ghadimi et al. [9]. found similar posterior atlas arch deficiencies in CGs and patients. Similar to Ghadimi et al. [9]., in our study, posterior arch deficiency had a low effect on the distinction between palatally impacted canines and controls.

Although dental anomalies had a more homogeneous structure in experiments 2 and 3, experiment 4 included individuals with different types of dental anomalies and different anomalies. Experiment 4 demonstrated that sella height median and the ratio of ID/STL were the most important factors in distinguishing between the other DAG group and the CG, respectively. In experiments 1, 2, and 3, several variables stood out in differentiating between anomalies and controls. Experiment 4 examined the coefficients of the variables; no variable was pronounced as much as in other experiments, and the variables with the highest coefficients did not have as high coefficients as in the other experiments. This situation is likely due to the high importance of different variables in different and multiple dental anomalies due to the heterogeneity of the distribution of dental anomalies in the sample.

From a clinical perspective, sella turcica bridging and vertebral malformations are diagnostic markers for identifying patients with congenitally missing teeth and palatally impacted canines, aiding treatment decisions. These abnormalities appear in early childhood, so

timely diagnosis by orthodontists is crucial. Recognizing these markers helps predict dental and skeletal anomalies, enabling preventative interventions. Orthodontists should understand craniofacial malformations beyond the maxillomandibular complex for a comprehensive diagnosis and treatment plan. Tooth agenesis causes functional and aesthetic issues from an early age, often necessitating orthodontic treatment or prosthetic tooth replacement [44].

If a palatally impacted canine is suspected, orthodontists may recommend extracting the deciduous canine or space expansion. Critical indicators for treatment include asymmetry in the maxillary canine's eruption, inappropriate crown position on a panoramic radiograph, congenitally teeth agenesis, size reduction, or a peg-shaped lateral incisor. Sella turcica bridging can also predict palatally impacted canines. Early detection and preventive treatment of impacted canines are critical, reducing treatment duration, cost, and effort [39].

## Conclusion

In summary, each prediction model obtained in the four experiments pointed to different variables as being the most important. The prominence of different variables in the model of each experiment shows how these features affect the dependent variable of each experiment and how they shape the predictive ability of the model. From a clinical point of view, these results may provide insights into the need to focus on specific characteristics for research in related fields. The assessment of sella turcica morphometrics and cervical vertebral malformations plays a critical role in facilitating the identification and management of dental anomalies, providing insights into potential dental abnormalities, and guiding clinical decision-making in orthodontic practice. LCR is used by orthodontists routinely for diagnosis and treatment planning; it can also be used as a prediction tool for dental anomalies. Early detection of skeletal anomalies can be used to forecast the presence of dental anomalies later in life, which will help the clinician adopt preventive measures.

The reference points at which evaluations are made have different definitions in the literature, so comparisons of findings must be more careful. Because our study used a specific age range, longitudinal data should be used in future studies to investigate data that can effectively differentiate dental anomaly-CG in varying age ranges.

## Abbreviations

LCR	Lateral Cephalometric Radiograph
STB	Sella Turcica Bridge
CV	Cervical Vertebrae
AI	Artificial Intelligence
CG	Control Group
PR	Panoramic Radiograph
TDAG	Total Dental Anomaly Group

DAGG Only Dental Agenesis Group  
 PICG Palatally Impacted Canine Group

#### Author contributions

MG: Conceptualization, methodology, acquisition of the data, data analysis, writing original draft preparation, reviewing, and editing. BBG: Acquisition of the data, writing-reviewing, and editing. MFS: data analysis, supervision, writing-reviewing, and editing.

#### Funding

The authors did not receive any funding from any organizations.

#### Data availability

The datasets used and/or analysed during the current study are available from the corresponding author on reasonable request.

#### Declarations

##### Ethics approval and consent to participate

The Institutional Review Board and Clinical Ethics Committee of the Recep Tayyip Erdogan University Medicine Faculty approved this retrospective clinical study (Registration number: 2022/36). Informed written consent was obtained for each patient routinely at the beginning of treatment, including consent to use patient records in scientific studies.

##### Consent for publication

Not applicable.

##### Competing interests

The authors declare no competing interests.

Received: 31 May 2024 / Accepted: 21 August 2024

Published online: 29 August 2024

#### References

- Leonardi R, et al. A sella turcica bridge in subjects with dental anomalies. *Eur J Orthod.* 2006;28(6):580–5.
- Shrestha GK, et al. The morphology and bridging of the sella turcica in adult orthodontic patients. *BMC Oral Health.* 2018;18(1):45.
- Kaya Y, et al. Sella turcica bridging and ponticulus posticus calcification in subjects with different dental anomalies. *Am J Orthod Dentofac Orthop.* 2021;159(5):627–34.
- Uğar DA, Semb G. The prevalence of anomalies of the upper cervical vertebrae in subjects with cleft lip, cleft palate, or both. *Cleft palate-craniofacial J.* 2001;38(5):498–503.
- Jankowski T et al. Sella Turcica Morphology on cephalometric radiographs and Dental Abnormalities-Is there any Association?-Systematic review. *Int J Environ Res Public Health.* 2021. 18(9).
- Macri M, et al. Assessments of prevalence of Ponticulus Posticus, Atlas posterior Arch Deficiency, Sella Turcica Bridging, Maxillary Canine Impaction, and associations among them in 500 CBCTs of Italian Orthodontic patients. *Front Dent Med.* 2021;2:708169.
- Sato D, Endo T. Size and bridging of the sella turcica in Japanese orthodontic patients with tooth agenesis. *Odontology.* 2020;108(4):730–7.
- Kjaer I. Sella turcica morphology and the pituitary gland-a new contribution to craniofacial diagnostics based on histology and neuroradiology. *Eur J Orthod.* 2015;37(1):28–36.
- Haji Ghadimi M, et al. Associations among Sella turcica bridging, atlas arcuate foramen (ponticulus posticus) development, atlas posterior arch deficiency, and the occurrence of palatally displaced canine impaction. *Am J Orthod Dentofac Orthop.* 2017;151(3):513–20.
- Karaman A, Cigerim SC, Kechagia N. Evaluation of the relationship between Sella Turcica Bridging and Dental anomalies. *J Dentistry Indonesia.* 2021;28(2):76–81.
- Meyer-Marcotty P, Reuther T, Stellzig-Eisenhauer A. Bridging of the sella turcica in skeletal class III subjects. *Eur J Orthod.* 2010;32(2):148–53.
- Antonarakis GS, Ghislanzoni LH, Fisher DM. Sella Turcica bridging and tooth agenesis in Children with Unilateral Cleft lip and palate. *Cleft Palate-Craniofacial J.* 2020;58(11):1382–8.
- Putrino A et al. *The Association between Ponticulus Posticus and Dental Agenesis: a retrospective study.* *Open dent J.* 2018. 12: p. 510–9.
- Guarnieri R et al. Predictive Analysis of Maxillary Canine Impaction through Sella Turcica Bridging, Ponticulus Posticus Calcification, and lateral incisor anomalies: a retrospective observational study. *Methods Protoc.* 2022. 5(6).
- Atilla AO, Ozturk T, Yagci A. Comparison of cervical vertebral anomalies and sella turcica bridging in different growth stages with various vertical skeletal growth patterns. *Surg Radiol Anat.* 2021;43(1):117–25.
- Buyuk SK, et al. A survey of ponticulus posticus: radiological analysis of atlas in an orthodontic population based on cone-beam computed tomography. *Niger J Clin Pract.* 2017;20(1):106–10.
- Sharma V, Chaudhary D, Mitra R. Prevalence of ponticulus posticus in Indian orthodontic patients. *Dentomaxillofac Radiol.* 2010;39(5):277–83.
- Kim MS. Anatomical variant of Atlas: Arcuate Foramen, Occipitalization of Atlas, and defect of posterior Arch of Atlas. *J Korean Neurosurg Soc.* 2015;58(6):528–33.
- Kononenko I. Machine learning for medical diagnosis: history, state of the art and perspective. *Artif Intell Med.* 2001;23(1):89–109.
- Prokhorenkova L et al. Nips., *CatBoost: unbiased boosting with categorical features.* *Advances in Neural Information Processing Systems* 31 (2018), 2018. 31.
- Hancock JT, Khoshgoftaar TM. CatBoost for big data: an interdisciplinary review. *J Big Data.* 2020;7(1):94.
- Elnour H, et al. Evaluation of shape and size of sella turcica using computerized tomography in Saudi populations. *Sch J Appl Med Sci.* 2020;8:2058–63.
- Sundareswaran S, Nipun CA. Bridging the gap: Sella Turcica in Unilateral Cleft lip and palate patients. *Cleft Palate Craniofac J.* 2015;52(5):597–604.
- Landis JR, Koch GG. The measurement of observer agreement for categorical data. *Biometrics.* 1977;33(1):159–74.
- Koo TK, Li MY. A Guideline of selecting and reporting Intraclass correlation coefficients for Reliability Research. *J Chiropr Med.* 2016;15(2):155–63.
- Leonardi R, et al. Skeletal anomalies and normal variants in patients with palatally displaced canines. *Angle Orthod.* 2009;79(4):727–32.
- Ali B, Shaikh A, Fida M. Association between sella turcica bridging and palatal canine impaction. *Am J Orthod Dentofac Orthop.* 2014;146(4):437–41.
- Gupta SPS, Rauniyar S. Association between Sella Turcica Bridging and Hypodontia - A Radiographic Study. *Europasian J Med Sci.* 2020;2(1):11–6.
- Saokar PC, Dinesh MR, Shetty A. A correlative study of sella turcica bridging and dental anomalies related to size, shape, structure, number and eruption of teeth. *J Orthod Sci.* 2022;11(1):2.
- Sobuti F, et al. Relationship between bridging and dimensions of sella turcica with classification of craniofacial skeleton. *Pol J Radiol.* 2018;83:e120–6.
- Magat G, Ozcan S, Sener. Morphometric analysis of the sella turcica in Turkish individuals with different dentofacial skeletal patterns. *Folia Morphol (Warsz).* 2018;77(3):543–50.
- Baidas LF, et al. Association of Sella turcica bridging with palatal canine impaction in skeletal class I and Class II. *Clin Cosmet Investig Dent.* 2018;10:179–87.
- Dasgupta P, et al. Sella Turcica bridging as a predictor of class II Malocclusion-An investigative study. *J Stomatol Oral Maxillofac Surg.* 2018;119(6):482–5.
- Alkofide EA. The shape and size of the sella turcica in skeletal class I, Class II, and Class III Saudi subjects. *Eur J Orthod.* 2007;29(5):457–63.
- Axelsson S, Storhaug K, Kjaer I. Post-natal size and morphology of the sella turcica. Longitudinal cephalometric standards for norwegians between 6 and 21 years of age. *Eur J Orthod.* 2004;26(6):597–604.
- Björk A, Skieller V. Normal and abnormal growth of the mandible. A synthesis of longitudinal cephalometric implant studies over a period of 25 years. *Eur J Orthod.* 1983;5(1):1–46.
- Grolinger K et al. *Challenges for MapReduce in Big Data.* in *2014 IEEE World Congress on Services.* 2014.
- Drosou M, et al. Diversity in Big Data: a review. *Big Data.* 2017;5(2):73–84.
- Omastova A, et al. Morphological types of sella turcica bridging and sella turcica dimensions in relation to palatal canine impaction: a retrospective study. *J Clin Pediatr Dent.* 2023;47(5):124–32.
- Leonardi R, Farella M, Cobourne MT. An association between sella turcica bridging and dental transposition. *Eur J Orthod.* 2011;33(4):461–5.
- Scribante A, et al. Sella turcica bridging and dental anomalies: is there an association? *Int J Paediatr Dent.* 2017;27(6):568–73.
- Siddalingappa D, et al. Sella Turcica Bridging and its Association with Dental anomalies. *Open Dentistry J.* 2021;15:473–8.
- Majeed O, Quadeer TA, Habib M. Relationship between Palatally Impacted canines and Sella Turcica Bridging. *JFDA.* 2018. 27(4).

44. Sobouti F, et al. Relationship between Craniovertebral Abnormalities and Maxillary lateral incisors agenesis: a case-control study. *Int J Dent*. 2022;2022:3389741.

### **Publisher's note**

Springer Nature remains neutral with regard to jurisdictional claims in published maps and institutional affiliations.